Use of Magnetic Torque for Removing Bias Momentum with Application to Skylab

WILLIAM LEVIDOW* AND JACK KRANTON†
Bellcomm, Inc., Washington, D.C.

In this paper an optimal control law is derived for the magnetic moment which, interacting with the earth's magnetic field, produces the torque required to remove (dump) an arbitrary bias momentum from a momentum exchange attitude controller. The optimization minimizes the electric energy needed to generate the magnetic moment. The optimal control law suggests a suboptimal control law that is simpler to implement and yet is near optimum in performance. The suboptimal control law involves sensing the stored angular momentum once per orbit. This law is evaluated for application on a spacecraft similar to the NASA Skylab flying in either of two attitude modes—long axis perpendicular to the orbital plane (POP mode) or long axis lying in the orbital plane (IOP mode). Minimum-weight air-coil and iron-core electromagnet designs are presented. For a 20-ft-diam air-coil design, the total coil and power supply weights are 134 lb for the POP mode and 366 lb for the IOP mode. System implementation would require adding to the attitude control system a magnetometer, the electromagnets, and a control amplifier to drive the magnet coils. The magnetometer can be placed so that it is not adversely affected by the magnetic field of the electromagnets.

Introduction

TO hold an earth orbiting spacecraft in an inertial attitude, a momentum exchange controller, for example inertia wheels or control moment gyroscopes (CMGs), must counteract the external torques that act on the spacecraft. The momentum exchange concept is based on the fact that in holding inertial attitude the change in spin angular momentum of the controller must equal the integral of the external torques. In a low Earth orbit the bias (unidirectional) components of the gravity gradient and aerodynamic torques cause momentum accumulation in the controller which if not removed (dumped) would cause momentum saturation. This paper deals with the problem of dumping the bias momentum by use of magnetic torque that is created by the interaction of an onboard magnetic moment with the Earth's magnetic field.

Among possible control laws for generating a magnetic moment for dumping, the one most generally proposed[1,2] constructs a magnetic moment $\mathbf{M}$ such that the magnetic torque is proportional to and directed opposite to that component of the stored angular momentum $\mathbf{H}$ lying in the plane perpendicular to the Earth's magnetic field $\mathbf{B}$. Then $\mathbf{M} = k(\mathbf{H} \times \mathbf{B})/|\mathbf{B}|^2$. A simplification suggested in a number of references[2-6] and currently used for momentum dumping of the Orbiting Astronomical Observatory[7] is to neglect the $|\mathbf{B}|^2$ term, since for a circular orbit it varies at most by a factor of 2 (i.e., in a polar orbit).

A further simplified version of this control has been suggested[2,4,8] for systems in which $\mathbf{M}$ is developed by three mutually orthogonal electromagnets. The simplification is achieved by providing a fixed, on-off magnetic moment along each spacecraft axis rather than a variable one. Threshold measurements of the components of $\mathbf{H}$ and $\mathbf{B}$ are combined in logical operations to command a fixed $\mathbf{M}$ most nearly in the direction defined by $\mathbf{H} \times \mathbf{B}$, and $\mathbf{M}$ is held fixed until one of its components is switched as the result of changes in either $\mathbf{H}$ or $\mathbf{B}$.

Instead of electromagnets, a gimbaled permanent bar magnet may be used. A regime has been described[9] in which the magnet is oriented along the direction defined by $\mathbf{H} \times \mathbf{B}$ when the magnitude of the projection of $\mathbf{H}$ on the plane perpendicular to $\mathbf{B}$ exceeds a threshold value. At other times, dumping is inhibited by aligning the magnet with $\mathbf{B}$.

In each of these schemes the magnetic torque is developed in the direction to decrease $|\mathbf{H}|$. Since the disturbance torques have cyclic as well as bias components, both $\mathbf{H}$ and the magnetic torque also contain cyclic components. The magnetic torque then sometimes aids and sometimes opposes the bias disturbance torques. Hence significant electric energy or magnet weight is devoted to shifting $\mathbf{H}$ in various directions rather than in dumping the bias component. This action to minimize $|\mathbf{H}|$ may be necessary if the momentum storage capacity of the controller is inadequate to handle the cyclic components, but it is inefficient for dumping bias momentum.

In this paper we deal directly with the bias momentum and derive an optimal control law for the $\mathbf{M}$ to cope with it. The optimization minimizes the electric energy needed to generate $\mathbf{M}$ to dump bias momentum. The optimal control can be implemented directly. However, it suggests a control law that is simpler to implement and yet is near optimum in performance. This control law is evaluated and electromagnet designs are given for possible application on a spacecraft similar to the Skylab on which attitude control is provided by CMGs. Momentum dump of the CMGs on the Skylab will be accomplished during orbital night by executing a sequence of maneuvers from the desired attitude such that the integral of the external torques over an entire orbit tends to zero. If magnetic torque were used, the need for such maneuvers would be eliminated, but at the expense of the hardware (weight and power) needed to generate $\mathbf{M}$.

Optimal Magnetic Moment Control Law

The torque $\mathbf{T}$ acting on a magnet of magnetic moment $\mathbf{M}$ in the earth's magnetic field $\mathbf{B}$ is

$$\mathbf{T} = \mathbf{M} \times \mathbf{B} \tag{1}$$

This torque acts on the spacecraft to which the magnet is

Received April 21, 1970; revision received July 16, 1970. This study was suggested by the interest of O. K. Garriott of the NASA Manned Spacecraft Center in the possible application of magnetic torque for attitude control of large manned spacecraft.

* Member of Technical Staff, Rotational Dynamics and Attitude Control Group, Apollo Applications Division.

† Supervisor, Rotational Dynamics and Attitude Control Group, Apollo Applications Division.

fixed. For proper dumping, the momentum change produced by the magnetic torque over an orbit must be equal and opposite to the bias momentum $\mathbf{H}_b$ during that orbit due to the gravity gradient and aerodynamic disturbance torques; that is,

$$\int_0^T (\mathbf{M} \times \mathbf{B})dt + \mathbf{H}_b = 0 \tag{2}$$

where T is the orbital period.

Since $|\mathbf{M}|$ is proportional to the magnetizing current, the electric power required, for a given magnet coil resistance, is proportional to $|\mathbf{M}|^2$. A reasonable objective in choosing $\mathbf{M}$ is to minimize

$$\int_0^T |\mathbf{M}|^2 dt$$

resulting in minimum electric energy for that orbit. The problem then is to choose $\mathbf{M}$ so as to minimize

$$\int_0^T \mathbf{M}'\mathbf{M}dt$$

subject to the constraint given by Eq. (2), where $\mathbf{M}'$ is the transpose of $\mathbf{M}$. This problem may be solved by the method of Lagrange multipliers to yield

$$\mathbf{M} = \left[\left(-\int_0^T \tilde{\mathbf{B}}^2 dt\right)^{-1} \mathbf{H}_b\right] \times \mathbf{B} \tag{3}$$

where $\tilde{\mathbf{B}}$ is the matrix equivalent to the vector cross product operation $\mathbf{B}\times$.

For this solution to be realizable the matrix in the parenthesis must be nonsingular. It will now be shown that this matrix is positive definite and hence nonsingular. Let $\mathbf{u}$ be an arbitrary time invariant vector. Then,

$$\mathbf{u}'\left(-\int_0^T \tilde{\mathbf{B}}^2 dt\right)\mathbf{u} = \int_0^T \mathbf{u}'[\mathbf{B} \times (\mathbf{u} \times \mathbf{B})]dt =$$

$$\int_0^T |\mathbf{B}|^2 |\mathbf{u}|^2 \sin^2\phi dt$$

where ϕ is the angle between $\mathbf{B}$ and $\mathbf{u}$. Except for an orbit coincident with the Earth's magnetic equatorial plane, the direction of $\mathbf{B}$ is not time invariant. Hence for any fixed $\mathbf{u}$, $\sin\phi$ cannot be zero over the entire interval $[0,T]$. In general, then, the above expression is positive for any $\mathbf{u}$ and the matrix is positive definite.

This result demonstrates the existence of an $\mathbf{M}$ given by Eq. (3) which over an orbit will dump an arbitrary bias momentum. The quantity within the brackets of Eq. (3) is a constant vector for the orbit, and $\mathbf{M}$ varies with time because of variations in $\mathbf{B}$. This solution for $\mathbf{M}$ could be implemented, but it requires knowledge of both $\mathbf{B}$ and $\mathbf{H}_b$ before the orbit is flown. Because these quantities are not precisely known in advance, and because of the computational requirement involved, the solution is not as attractive as the following control law which it suggests.

Suboptimal Implementation of Control Law

Let $\mathbf{M}$ be defined over an orbit as

$$\mathbf{M} = k\mathbf{H}_s \times \mathbf{B} \tag{4}$$

where $\mathbf{H}_s$ is the CMG momentum (computed from gimbal angles) sampled at the beginning of the orbit. $\mathbf{M}$ varies over the orbit because of variations in $\mathbf{B}$. If the CMG system is initialized such that $k\mathbf{H}_s$ equals the vector in the brackets of Eq. (3), then the two solutions are identical. This can be accomplished by both adjustment of the CMG gimbal angles at the initial sampling and selection of the scale factor k. With this initialization, exactly $\mathbf{H}_b$ is dumped in the following orbit.

If the variation of $\mathbf{B}$ from orbit to orbit were identical, then $\mathbf{H}_b$ would be dumped each orbit and $\mathbf{H}_s$ would be identical at each sampling (the cyclic component of the CMG momentum does not affect the once per orbit sample value). However, $\mathbf{B}$ is not identical from orbit to orbit because the Earth's rotation and orbital regression varies the direction of the Earth's magnetic dipole relative to the orbital plane. As a result, a momentum somewhat different from $\mathbf{H}_b$ is dumped for some orbits. Simulation results are presented later which show that this causes $\mathbf{H}_s$ to vary within a small bounded region determined by the scale factor k. Furthermore, even if $\mathbf{H}_s$ is not initialized properly, it converges to within the same region in a few orbits; it automatically adjusts for orbit changes in $\mathbf{B}$ and $\mathbf{H}_b$ to provide the proper $\mathbf{M}$ for dumping.

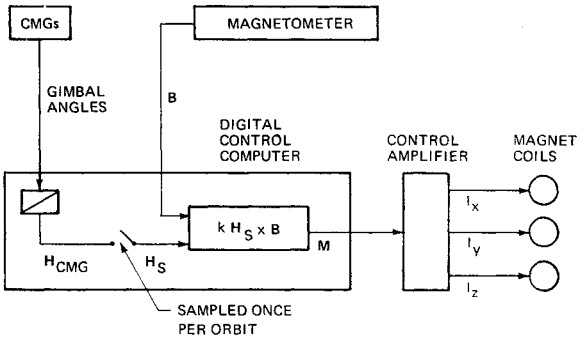

Fig. 1 Magnetic dump system.

$\mathbf{H}_s$ can be made to converge to a different region by setting $\mathbf{M} = k(\mathbf{H}_s - \mathbf{H}_0) \times \mathbf{B}$ where $\mathbf{H}_0$ is the desired shift in the region.

Except for the change in the profile of $\mathbf{M}$ due to the change in $\mathbf{B}$ from orbit to orbit, the control law [Eq. (4)] requires minimum energy from the power supply.

A block diagram of the magnetic dump system is shown in Fig. 1. Equipment required are the magnetometer to measure the Earth's magnetic field, the electromagnets, and the control amplifier to control the current to the magnet coils. $\mathbf{H}_s$ is obtained by sampling the CMG momentum. The impact on the control computer is of a software nature and the computational time required is small.

Control Law Simulation

The control law $\mathbf{M} = k(\mathbf{H}_s \times \mathbf{B})$ was simulated for possible use on a long duration, Earth-orbiting spacecraft similar to the Skylab (Fig. 2) with a telescope experiment canister gimbal mounted along the Z axis for celestial viewing. The spacecraft was assumed to fly in a 220-naut-mile, 35°-inclination circular orbit and to derive power from solar-cell panels oriented perpendicular to the Earth-sun line. For this study the sun was considered to lie in the orbital plane, resulting in the maximum aerodynamic bias momentum (225 ft-lb-sec)

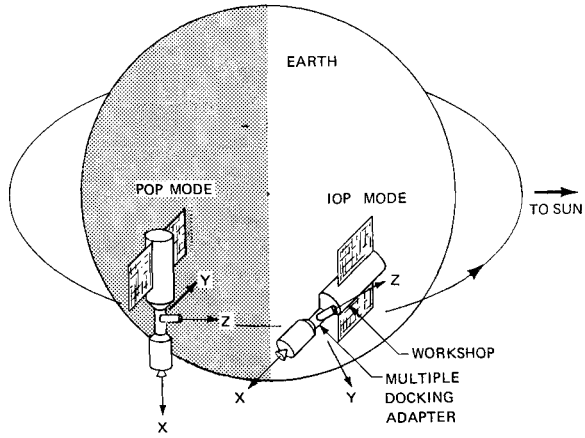

Fig. 2 Attitude modes.

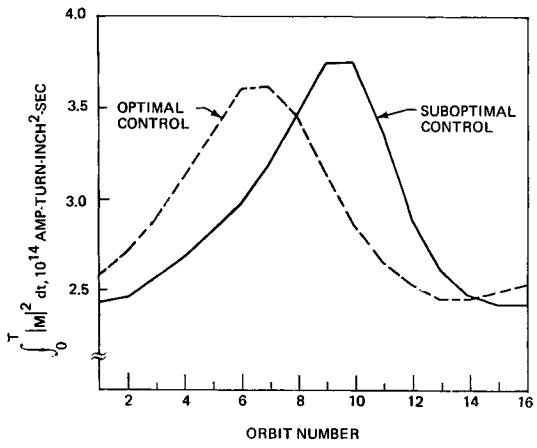

Fig. 3 Per orbit electric energy comparison.

because of the effect of the diurnal bulge on the aerodynamic torque.

Two inertial‡ attitude modes were considered—POP (long axis perpendicular to the orbital plane) and IOP (long axis in the orbital plane). For the POP mode, the bias momentum is primarily aerodynamic. The gravity gradient bias momentum resulting from misalignment of the principal and geometric axes can be reduced to 30 ft-lb-sec by a small Y axis maneuver. Both bias momentum vectors lie in the orbital plane.

For the IOP mode, the gravity gradient bias momentum vector lies in the orbital plane and is maximized when the Z principal axis lies 45° out of the orbital plane. The aerodynamic bias momentum vector is perpendicular to the orbital plane.

The estimated principal moments of inertia (slug-ft^2) for the spacecraft were I_x = 634,400, I_y = 4,220,600, and I_z = 4,112,900. The corresponding total aerodynamic and gravity gradient bias momenta (ft-lb-sec) per orbit along the vehicle coordinate axes were (0,255,0) for the POP mode and (−575,−160,−160) for the IOP mode.

For both modes the simulation consisted of setting $k\mathbf{H}_s$ for the first orbital equal to the value within the brackets of Eq. (3). At each successive sampling, $\mathbf{H}_s$ was incremented by

$$\Delta\mathbf{H}_s = \mathbf{H}_b + \int_0^T (\mathbf{M} \times \mathbf{B})dt$$

Each simulation was run for 16 orbits during which time the Earth makes approximately a full rotation. It was found that a wide range of scale factor k provided satisfactory dump operation.

Simulations were also conducted in which $\mathbf{H}_s$ was initialized to the null vector. Values of k ranging from 7×10^4 to 12×10^4 produced, after a few orbits, the same $\mathbf{M}$ profile as when $\mathbf{H}_s$ had been properly initialized. With $k = 9.5 \times 10^4$ and $\mathbf{H}_s$ given in ft-lb-sec, $\mathbf{B}$ in lines/in.^{2}, and $\mathbf{M}$ in amp-turn-in.^{2}, the magnitudes of the variation of $\mathbf{H}_s$ over 16 orbits were 48§ ft-lb-sec in the POP mode and 363 ft-lb-sec in the IOP mode. Similar results were obtained for other values of k, which indicates that convergence of $\mathbf{H}_s$ to a small bounded region is insensitive to the value of k. Between samplings, however, the variation of CMG momentum is larger because of the cyclic components of the aerodynamic and gravity gradient torques.

Figure 3 compares the electric energy requirements per orbit for the optimal and the suboptimal control laws as determined from a simulation of 16 orbits. As anticipated, the difference in total electric energy over the 16 orbits is small; in fact it was not discernible. The energy peak for the suboptimal control lags that of the optimal control, and the energy used by the suboptimal control is less than that of the optimal control in some orbits. This occurs because the optimal control law dumps precisely $\mathbf{H}_b$ each orbit, even when the $\mathbf{B}$ profile for that orbit results in large values of $|\mathbf{M}|$ and energy. During these unfavorable orbits, the suboptimal control dumps less than $\mathbf{H}_b$ and uses less energy. This results in an orbit by orbit accumulation of bias momentum which causes the suboptimal control to dump more than $\mathbf{H}_b$ in later orbits with an associated increase in energy. This accounts for the separation of the peaks in the energy curves.

As discussed later, the wave shape of $|\mathbf{M}|$, in particular its maximum value M_m and its rms values M_d and M_n during orbital day and night, determines the weight penalty of magnetic dumping. The greatest values over 16 orbits demanded by the suboptimal control law are given in Table 1.

Magnet Designs

Both air-coil and iron-core electromagnet designs were considered. Each type may be configured as a single gimbaled magnet (with a two-degree-of-freedom mechanism) or as three fixed orthogonal magnets. In all four designs the magnitude of the magnetic moment of each magnet is proportional to coil current. For the three-magnet designs, $\mathbf{M}$ is controlled by apportioning current among the three coils; the electric power required is proportional to $|\mathbf{M}|^2$. The same power is demanded if one of the same magnets is used in a gimbaled design, but only one-third of the magnet weight is required. However, for minimum total weight of power supply and magnets, the two coil designs will differ.

If magnetic dumping is done continuously, battery power is required during orbital night. During orbital day, however, solar cells can power the magnet and also recharge the batteries. For all four magnetic designs, the minimum total weight of power supply and conductor (total weight of three coils for the three-magnet designs) occurs if the power supply weight equals the conductor weight. This results in the following design relationships for minimum system weight:

Air-coil designs:

$$\text{conductor weight} \propto (K_d M_d^2 + K_n M_n^2 + K_a M_m^2)^{1/2}/D$$

Iron-core designs:

$$\text{conductor weight} \propto (K_d M_d^2 + K_n M_n^2 + K_a M_m^2)^{1/2}/M_m^{1/3}$$

$$\text{iron core weight} \propto M_m$$

where M_m = maximum value of $|\mathbf{M}|$; M_d, M_n = rms values of $|\mathbf{M}|$ during orbital day and night; K_d, K_n = constants dependent upon solar array and battery characteristics, and K_n also depends upon the length of orbital night and day; K_a = specific weight of the control amplifier, lb/w (K_a for a three-magnet design is approximately three times that for a gimbaled magnet design because three amplifier channels are required); and D = air-coil diameter. Detailed coil design equations are given in Ref. 10.

Minimum weight designs carried out for the magnetic moment data of Table 1 are shown in Table 2. A 20-ft-diam air-coil was chosen because it fits within the Skylab skin. For other diameters the maximum powers and weights can be determined from the fact that they are inversely proportional to the coil diameter. However, these are the minimum weights

Table 1 Magnetic moments, 10^6 amp-turn-in.^{2}

Mode	M_m	M_d	M_n
POP	4.92	4.02	3.59
IOP	14.20	10.60	9.60

‡ For the purpose of this study the attitude was considered inertial for the time span of several orbits.

§ The present CMG system has a momentum storage capacity of nearly 12,000 ft-lb-sec.

Table 2 Minimum weight magnet designs, $\mathbf{M} = k\mathbf{H}_s \times \mathbf{B}$ control law, continuous dumping

Air-coil designs (20-ft-diam coil)	Gimbaled		Three orthogonal units[a]	
	POP	IOP	POP	IOP
Maximum amp-turns	109	314	109	314
Turns × conductor area, in.^{2}	0.141	0.381	0.092	0.251
Current density, amp/in.^{2}	775	825	1190	1250
Maximum power, w	47	144	72	217
Copper weight, lb	34	92	67	183
Power supply weight, lb	34	92	67	183
Total weight, lb (copper + power supply)	68	184	134	366
Iron-core designs (45% nickel permalloy core)				
Core length, ft	6.0	8.5	6.0	8.5
Core length/diam	30	30	30	30
Core weight, lb (each)	95	274	95	274
Maximum amp-turns	4360	6190	4360	6190
Turns × conductor area, in.^{2}	5.62	7.56	3.66	5.0
Current density, amp/in.^{2}	775	820	1190	1240
Maximum power, w	18	40	28	61
Copper weight, lb	14	26	27	52
Power supply weight, lb	14	26	27	52
Total weight, lb (copper + power supply + cores)	123	326	339	926

[a] Power and copper weight are total for three coils.

for a 20-ft-diam coil design.¶ The power supply weight includes batteries, solar array, and control amplifier. The copper weight** does not include weight of insulation or winding forms. Although the total copper and power supply weights for the three-coil designs are almost twice that for the single-gimbaled-coil designs, the additional weight and complexity of the gimbal mechanism must be considered in comparing the two designs. Also, a large volume of space is required to accommodate the movement of the gimbaled coil.

The iron-core designs are for a core material of 45% nickel permalloy operating at a maximum flux density of 1 weber/m^2 and with a chosen core length/diameter ratio (L/D) of 30. The conductor and power supply weights, although minimized for this L/D, drop rapidly as the L/D increases. The iron-core weight, which predominates, is not sensitive to L/D. The weights for the three-magnet designs are approximately three times those for the single-magnet designs because three iron cores are required.

It is clear from Table 2 that air coils are preferred. Further, in view of the complexity introduced by a gimbal design, the single-coil design is less attractive than the three-coil design.

The effect of the required magnetic moment on the magnetic field in the vicinity of the Skylab must be considered in locating the magnetometer to measure the Earth's magnetic field. For the 20-ft-diam air coils, Table 3 shows the maximum field strength along the coil axis in percent of the Earth's magnetic field at the magnetic equator. If the coils are located at the aft end of the workshop (Fig. 2), the magnetometer can be located at a distance of 3 coil diameters in the Multiple Docking Adapter module. For the IOP mode, the maximum field strength produced there by the magnetic moment is 1.1% of the Earth's magnetic field. This will not adversely affect the dump operation.

Table 3 Maximum coil field strength in percent of Earth's magnetic field

Mode	Coil diameters from coil center			
	0	2	3	4
POP	86	1.2	0.38	0.17
IOP	250	3.6	1.1	0.48

Although the design method would have to be revised, it is not necessary that the three-magnet design comprise three identical magnets. It is more economical to construct larger magnets on the spacecraft axes of greatest required magnetic moment.

The portion of the weights of Table 2 attributable to the solar array and batteries is conservative for, as shown in Fig. 3, some orbits during an Earth's rotation have a much reduced electric energy demand. Hence during parts of the mission some of the battery and solar array capacity can be diverted to other uses.

Constrained Magnetic Moment

Since the required iron-core weight W_c is directly proportional to M_m, an attempt was made to decrease W_c by simulating the control law with an upper limit placed on $|\mathbf{M}|$. This resulted in a more nearly constant $|\mathbf{M}|$, since greater dumping action was required during periods when $|\mathbf{M}|$ previously was small. It was found that adequate dumping still occurred if $|\mathbf{M}|$ was limited to 85% of its unconstrained value. This allowed a 15% reduction in W_c, which was the major weight in the iron-core magnet designs, and a 15% reduction in weight of the control amplifier in all designs. There was little weight savings if air coils are used with a constrained $|\mathbf{M}|$, because the rms values remained nearly the same.

If magnetic dumping is done only during orbital day, batteries are not needed if the solar cells are sized to supply peak power. In this case it may be advantageous to select a control law which results in a constant magnitude of $\mathbf{M}$, with only its direction changing.

To study day-only dumping with constant $|\mathbf{M}|$, the control law with a limited maximum $|\mathbf{M}|$ was applied only during the 220° orbital day. A constant $|\mathbf{M}|$ 30% higher than that for day and night unconstrained dumping was found adequate. When minimum weight design equations developed[10] for day-only dumping with constant $|\mathbf{M}|$ were applied to the above results, the total weight of the solar array, control amplifier, and copper coils for the three 20-ft-diam air-coil designs were 153 lb for the POP mode and 441 lb for the IOP mode. But these weights are, respectively, 14% and 21% larger than the weights with an unconstrained $|\mathbf{M}|$. Similarly, for the iron-core designs, any savings in battery weight is clearly offset by a 30% increase in W_c. However, for higher altitude orbits with larger minimum orbital day this day-only dumping scheme may have a weight advantage.

Summary

A control law has been devised for determining the required magnetic moment profile over the orbit for CMG bias momentum dumping. Except for the small effect of orbit-to-orbit variations in the Earth's magnetic field, this control law minimizes the electric energy drawn from the power supply.

¶ To use Table 2, either the maximum current, turns, or conductor area can be chosen, consistent with a reasonable physical design. Choosing one determines the remaining two.

** A 30% savings in coil conductor and power supply weight can be realized if the coil conductors are made of aluminum instead of copper.

System implementation requires adding a magnetometer, a control amplifier, and the electromagnet to the attitude control system. A single gimbaled magnet or three fixed magnets, of air-coil or iron-core construction, may be used. In all cases, the total weight of conductor and power supply (solar array, batteries, and control amplifier) is a minimum if the conductor weight equals the power supply weight.

Although the total weight of magnet plus power supply is smaller for a gimbaled design, the additional weight and complexity of the gimbal mechanism and the space required to accommodate the moving magnet make the three-magnet design, in particular the air coils, more attractive.

Placing an upper bound on $|\mathbf{M}|$, the magnitude of the magnetic moment, allows an iron-core weight savings of 15%, but results in little weight savings for air-coil designs. Day-only dumping with a constant $|\mathbf{M}|$ eliminates the need for battery capacity, but a larger magnet size is required because of the reduced dumping time.

References

[1] White, J. S., Shigemoto, F. H., and Bourguin, K., "Satellite Attitude Control Utilizing the Earth's Magnetic Field," TN D-1068, Aug. 1961, NASA.

[2] Brown, S. C., "An Analytical Comparison of Some Electromagnetic Systems for Removing Momentum Stored by a Satellite Attitude Control System," TN D-2693, March 1965, NASA.

[3] Wheeler, P. C., "Magnetic Attitude Control of Rigid, Axially Symmetric, Spinning Satellites in Circular Earth Orbits," CR-313, Oct. 1965, NASA.

[4] Abbott, J. K., "Momentum Unloading Systems—Design of Magnetic Unloading Actuators," N67-36678, Jan. 1967, Royal Aircraft Establishment, Farnborough, England.

[5] Buckingham, A. G., "A Method of Attitude Control Utilizing the Earth's Magnetic Field for Space Vehicles," Rept. AA-2333, 1961, Westinghouse Electric Corp., Air Arm Division, Baltimore, Md.

[6] Hart, L. R. et al., "Application of Magnetic Torquing for Desaturation of Control Moment Gyros in Space Vehicle Control," TR AFFDL-TR-67-8, June 1967, Westinghouse Defense and Space Center, Baltimore, Md.

[7] Olsen, R., "OAO Magnetic Unloading System Performance in the Presence of a Realistic Earth Field," Rept. SYST-252R-7.0, May 1968, Grumman Aircraft Engineering Corp., Bethpage, N.Y.

[8] Blakemore, D. J., "Magnetic Torquing Scheme," *AIAA Journal*, Vol. 1, No. 8, Aug. 1963, pp. 1888–1889.

[9] Adams, J. J. and Brissenden, R. F., "Satellite Attitude Control Using a Combination of Inertia Wheels and a Bar Magnet," TN D-626, Nov. 1960, NASA.

[10] Levidow, W., "Use of Magnetic Torque for CMG Momentum Management," TM 69-1022-8, Dec. 1969, Bellcomm, Inc., Washington, D.C.

OCTOBER 1970 J. SPACECRAFT VOL. 7, NO. 10

Design of an Optimal-Adaptive Digital Autopilot

N. N. PURI*

Rutgers University, New Brunswick, N.J.

The heart of this autopilot design for the flight path control of an aerospace vehicle is a digital computer with three software subroutines for identification, optimal synthesis, and digital compensation. Vehicle motion is described by linear differential equations whose parameters change over a very wide range during the flight and are unknown except for some a priori guess. An identification algorithm based upon discrete orthogonal functions is used to identify the flight motion parameters. An optimization algorithm based upon quadratic performance index determines the closed-loop characteristic polynomial, which when combine with identified flight motion parameters yields the suitable compensation.

Nomenclature

$A_k^{(j)}$	= Fourier coefficients of $x_j(n)$ with respect to orthogonal set $\varphi_k(n)$
$a_n^{(j)},b_k^{(j)}$	= coefficients of z^{-n} in the series expansion of the numerator and denominator, respectively, of $G^{(j)}(z), n = 0,1,2,\ldots$
$B_k^{(j)}$	= Fourier coefficients of $u_j(n)$
β	= performance index parameter
c_k	= coefficients of z^k and z^{-k} in $F(z)$
$D(s),D(z)$	= autopilot transfer function
$G^{(j)}(z),D^{(j)}(z)$	= vehicle and autopilot transfer functions computed from $\{x_j(n)\}_0^{2N}$ and $\{u_j(n)\}_0^{2N}$
$F(z)$	= optimization polynomial
$G(s),G(z)$	= vehicle transfer function
I	= performance index
$2N$	= number of samples required for vehicle dynamic identification
T	= identification time
$u(t)$	= vehicle input or control signal, measured
$u^*(t)$	= vehicle input, without noise
$x(t),x^*(t)$	= vehicle output, measured and without noise
$x_j(n),u_j(n)$	= sampled values of $x(t)$ and $u(t)$ at $t = (j + n)T/2N \quad j = 0, \ldots, \infty, n = 0, \ldots, 2N$
$v(t),\omega(t)$	= input, output noise
$\{\varphi_k(n)\}_0^\infty$	= set of orthogonal functions, $n = 0, \ldots, \infty$
$\Phi_k(z)$	= Z transform of $\varphi_k(n)$
s	= Laplace transform variable
z	= Z transform variable = e^{-sT}
$\nabla(z)$	= characteristic polynomial of closed-loop transfer function

Introduction

INTEREST in digital autopilot design has increased in recent years due to rapid advances in digital technology. A conventional autopilot is an analog device that provides some fixed compensation based upon assumed vehicle dynamics and environment. The necessity of providing guidance and navigation functions for aerospace vehicles makes it very attractive to combine all of these functions in a control digital computer. Since the autopilot function in a digital

Received November 11, 1969; revision received May 8, 1970.

* Professor of Electrical Engineering, Department of Electrical Engineering.